JOURNAL OF CATALYSIS 51, 269–277 (1978)

Surface Characterization of Silica–Aluminas by Photoelectron Spectroscopy

C. DEFOSSÉ,[1] P. CANESSON,[2] P. G. ROUXHET,[3] AND B. DELMON

Groupe de Physico-Chimie Minérale et de Catalyse, Université Catholique de Louvain, Place Croix du Sud 1, B-1348 Louvain-la-Neuve, Belgium

Received March 15, 1977; revised October 7, 1977

Structural organization and surface acidity of a series of silica–alumina gels covering the range from 100 to 0% SiO_2 have been investigated by photoelectron spectroscopy. No superficial segregation of either SiO_2 or Al_2O_3 is observed and the existence of a distinct alumina phase below 30% SiO_2, as suggested earlier, is further supported by the appearance of an energy-loss peak. Models are presented for the interpretation of the quantitative XPS determination of surface acidity. Close comparison is made between XPS acidity results and those obtained by ir spectroscopy on the same series and a good agreement is observed.

INTRODUCTION

The surface acidity of silica–alumina gels has been thoroughly studied by monitoring the adsorption of appropriate molecules, e.g., H-bond acceptors, nitriles, pyridine, with a suitable technique such as infrared spectroscopy (*1–8*).

The infrared spectra of adsorbed pyridine allow one to detect protonic and nonprotonic acid sites and have been used to study the relationship with various parameters such as the chemical composition of the adsorbant and the activation temperature.

The present work deals with an XPS study of the adsorption of pyridine on a series of silica–alumina gels. It aims at comparing XPS with ir spectroscopy as a technique for studying the adsorption of probe molecules. It was also expected that data on the surface composition of the gels, as revealed by XPS, could yield useful information on the structural organization of the solid.

EXPERIMENTAL

Materials

The synthesis of the silica–alumina series covering the range from pure silica to pure alumina is described elsewhere (*3*). Their surface and catalytic properties have recently been reviewed (*9*). Samples are identified by the sign SA- followed by their SiO_2 weight percentage.

Pyridine (Merck p.a.) was distilled *in vacuo* before use, thoroughly outgassed, and stored on an activated 5A molecular sieve.

Experimental Procedure

Samples. Four samples were studied for each composition:

Bk 25 refers to the so-called "blank" untreated samples.

[1] Candidate, Fonds National de la Recherche Scientifique, Belgium.

[2] Present address: Laboratoire de Chimie XI, UERSFA, Avenue du Recteur Pineau 40, F-86022 Poitiers, France.

[3] To whom reprint requests should be addressed.

0021-9517/78/0512-0269$02.00/0

Bk 550 corresponds to the blank samples outgassed at 550°C for 16 hr under a dynamic vacuum of 10^{-5}–10^{-6} Torr and sealed off in a glass vial.

Py 25 was obtained by contacting at 25°C for 30 min the samples outgassed at 550°C with the room-temperature vapor pressure of pyridine. After pyridine adsorption, samples were further outgassed *in vacuo* at 25°C for 1 hr and an aliquot was sealed off under vacuum in a lateral vial.

Py 100 was obtained from the remaining part of the previous sample Py 25 by further outgassing at 100°C for 1 hr, after slowly increasing the temperature from 25 to 100°C. This portion was sealed off in a second vial.

All samples except the Bk 25 were stored at liquid nitrogen temperature overnight before XPS analysis.

XPS analysis. The procedure used has been described in detail elsewhere (*10*). Spectra were recorded at −90°C and at room temperature with a Vacuum Generators ESCA 2 equipped with a glove box. Signal to noise ratios were similar to those reported in Ref. (*10*).

RESULTS AND DISCUSSION

Line Positions

Gold referencing was not used, since evaporation of gold onto the sample would possibly modify the surface and cause the desorption of pyridine. The O_{1s} and C_{1s} lines cannot be used for this purpose, as they cannot be considered as sufficiently reliable.

Concerning the Si_{2p} line, successfully used earlier (*10*), Fig. 1 shows that, for samples SA-20 to SA-0, there appears an unexpected broad and complex satellite line which is partially superimposed on the Si_{2p} line and the intensity of which increases with the alumina content. Therefore, the simple and symmetrical Al_{2p} level was chosen as reference, the binding energy

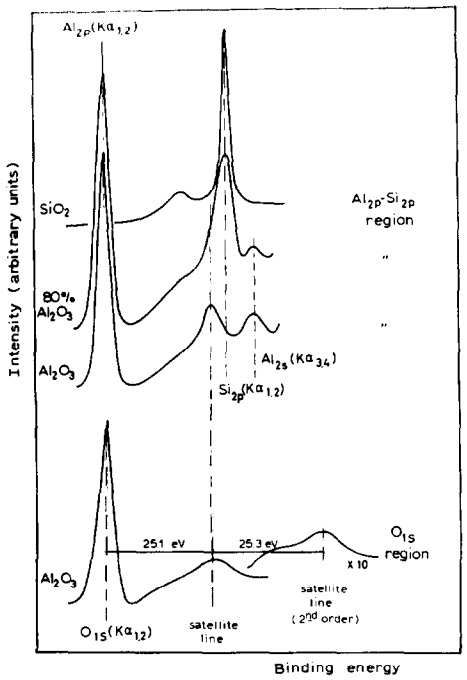

FIG. 1. Photoelectron spectra of the Al_{2p}–Si_{2p} and O_{1s} regions showing the presence, below 30% SiO_2, of a satellite for O_{1s} and Al_{2p} peaks.

of which was arbitrarly fixed at 0.0 eV. Having an internal reference allowed us to obtain a binding energy precision of 0.4 eV for the N_{1s} line and 0.2 eV for the others (*11*). Almost identical results were obtained when recording the spectra at −90°C or at room temperature: Therefore all results reported in this work are the average of the values obtained for the two temperatures.

The Si_{2p} and O_{1s} positions with respect to the Al_{2p} reference line show no systematic difference between the four types of pretreatment and no dependence on the silica content; the average valucs are, respectively, equal to 27.9 ± 0.1 and 457.3 ±0.1 eV.

In an earlier study of pyridine adsorption by HY zeolites (*10*), the position of the N_{1s} line referenced to the Si_{2p} line was shown to be dependent on the nature of the adsorption sites, i.e., Lewis or Brønsted. For the considered silica–alumina series,

it is known (*3*) that Brønsted and Lewis acidities coexist in the composition range 90–30% SiO_2, but below 30% the former no longer exists. Therefore the position of the N_{1s} level of chemisorbed pyridine (Py 100) was expected to be different between the 90–30% and the 30–0% SiO_2 ranges. No such shift is actually observed, and the average N_{1s} position with respect to the Al_{2p} reference line is equal to 326.3 $\pm$0.2 eV.

A possible explanation is the very large width ($\sim$4 eV) of the N_{1s} signal, which could possibly obscure an eventual shift. Such a large width is partly due to the insulating character of the sample, but it probably also reflects a rather large spread in acid site strength, especially when compared to the zeolites. As a result, XPS failed to distinguish qualitatively between Lewis and Brønsted acidities in silica–aluminas, contrary to what was observed for zeolites.

Line Intensities

XPS line intensities are affected by several factors that are very hard to estimate, namely, photon flux, analyzer luminosity, detector efficiency, and superficial carbon contamination, the latter being probably very important. Therefore all intensity measurements must be reported as intensity ratios between the line of interest and a reference line belonging to the sample, which has been chosen as the Al_{2p} line.

C_{1s} Line

C_{1s} contributions originating from contamination and adhesive tape are important enough to obscure the contribution of adsorbed pyridine and therefore preclude any quantitative interpretation.

O_{1s} Line

For elements belonging to the bulk of the sample, the intensity ratio is related to the concentration ratio by the following relationship:

$$\frac{Ix}{IR} \simeq \frac{i_x}{i_R}\frac{C_x}{C_R}, \qquad (1)$$

where Ix/IR is the experimental intensity ratio between line x and reference line R; C_x/C_R is the atomic concentration ratio; the ratio i_x/i_R is a constant, provided there is no matrix effect, and is a formal transcription for $\sigma_x\lambda_x/\sigma_R\lambda_R$, where σ is the photoelectric cross section and λ the mean free path.

The correlation between I Al_{2p}/I O_{1s}, averaged over the four types of pretreatment, and the ratio C_{Al}/C_O, calculated for the anhydrous silica–aluminas, provides a value of the $i_{O_{1s}}/i_{Al_{2p}}$ ratio equal to 5.6 $\pm$ 0.3, while values of 4.6 and 3.7 have been reported by Nefedov *et al.* (*12*) and Wagner (*13*), respectively. This discrepancy most probably arises from the fact that, the kinetic energy of the two lines being very different, the detector efficiency and analyzer luminosity are different and the experimental $i_{O_{1s}}/i_{Al_{2p}}$ ratios might substantially differ according to the commercial instruments used.

N_{1s} Line

Blank samples Bk 550 display a residual N_{1s} line, the position of which is not significantly different from the position observed after adsorption of pyridine. The nitrogen retained on these samples may be due to decomposition of nitrogen-containing species originating from the buffer solution used for the synthesis or adsorbed during storage in the laboratory. The values of the intensity ratio I N_{1s}/I Al_{2p} for the blank samples are not negligible with respect to the ratios measured after adsorption of pyridine.

As the aluminum content varies throughout the whole series, the N_{1s} intensity data have been normalized; they are given in

TABLE 1

Normalized N_{1s} Intensity Ratios from the Relation $(IN_{1s}/I\mathrm{Al}_{2p})C_{\mathrm{Al}}$

SA-	Bk 550	Py 25	Py 100	Py 25 − Bk 550	Py 100 − Bk 550	Py 25 − Py 100
100	0.000	—	0.000	—	0.000	—
90	0.031	0.098	0.057	0.067	0.026	0.041
80	0.050	0.118	0.097	0.068	0.047	0.021
70	0.023	0.119	0.067	0.096	0.044	0.052
60	0.020	0.125	0.083	0.105	0.063	0.042
50	0.041	0.151	0.110	0.110	0.069	0.041
40	0.041	0.179	0.166	0.138	0.125	0.013
30	0.055	0.195	0.173	0.140	0.118	0.022
20	0.078	0.184	0.169	0.106	0.091	0.015
10	0.070	0.158	0.138	0.088	0.068	0.020
0	0.029	0.121	0.113	0.092	0.084	0.008

Table 1 as $I\ \mathrm{N}_{1s}\ C_{\mathrm{Al}}/I\ \mathrm{Al}_{2p}$, where C_{Al} is expressed in g-atoms/100 g.

The differences Py 25 − Bk 550 and Py 100 − Bk 550 correspond to a minimum estimate of the contribution of adsorbed pyridine to the XPS spectrum. It should be noted that no pyridine remains adsorbed on the pure silica (SA-100) after outgassing at 100°C; it is therefore concluded that this treatment desorbs all the physically adsorbed and H-bonded species, the amount of which decreases as the SiO_2 content decreases (Py 25 − Py 100). On the other hand, the difference of intensity ratios Py 100 − Bk 550 is an estimate of the amount of pyridine chemisorbed on Lewis and Brønsted sites.

Basis of a Quantitative Interpretation of Acidity Measurements by XPS

Using line intensities of chemisorbed pyridine to obtain information concerning the acidity requires special caution: While the N_{1s} photoelectrons ejected from the pyridine molecules adsorbed on the external surface do not undergo inelastic processes if the effect of a contamination overlayer is neglected, photoelectrons chosen as standards, namely, those originating from the Al_{2p} level, do suffer such processes, so that only a fraction of them will effectively reach the detector. Consequently the apparent acid site concentration D', deduced from XPS line intensities, is greater than the true concentration D and

$$D = D'r = \frac{I\ \mathrm{N}_{1s}}{I\ \mathrm{Al}_{2p}} \frac{i_{\mathrm{Al}_{2p}}}{i_{\mathrm{N}_{1s}}} r, \qquad (2)$$

with $r < 1$.

Estimation of r is possible using geometrical models which simulate the actual porous solid to an aggregate of elementary particles. The size of these particles has no relationship with the size of the grains of the investigated sample but is chosen so that the surface to mass ratio of the elementary particles of the model is equal to the surface area S of the actual sample.

The three following models illustrated in Fig. 2 were examined:

sheets of thickness $t = 2/(\rho S)$ separated by an empty space of negligible thickness and perpendicular to the escape direction Z, ρ being the density of the silica–alumina considered.

cubes of edge $a = 6/(\rho S)$ with the threefold symmetry axis parallel to the escape direction Z.

spheres of radius $R = 3/(\rho S)$.

Sheets. The intensity of the N_{1s} line of adsorbed pyridine may be expressed by the

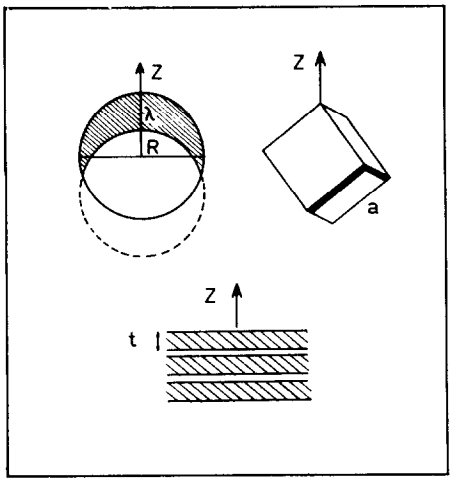

FIG. 2. Schematic representation of the various models used for correcting acidity measurements.

following relationship:

$$I\,N_{1s} = \sigma_{N_{1s}} n_N{}^s A \times [1 + 2\sum_{j=1}^{\infty} \exp(-jt/\lambda_{N_{1s}})], \quad (3)$$

where $n_N{}^s$ is the amount of pyridine adsorbed per unit area; A is the area hit by the X-ray beam; and $\exp(-jt/\lambda_{N_{1s}})$ represents the contribution of pyridine adsorbed on the lower face of the jth sheet or on the upper face of the $(j + 1)$th sheet.

The intensity of the Al_{2p} line is given by

$$I\,Al_{2p} = \sigma_{Al_{2p}} C_{Al}{}^v A \int_0^{\infty} \exp(-x/\lambda_{Al_{2p}})dx = \sigma_{Al_{2p}} C_{Al}{}^v A \lambda_{Al_{2p}}, \quad (4)$$

where $C_{Al}{}^v$ is the aluminum concentration in g-atoms per unit volume. For the model considered, the concentration of acid sites, in number of sites per Al atom, is given by

$$D = n_N{}^s 2A/C_{Al}{}^v At = 2n_N{}^s/C_{Al}{}^v t. \quad (5)$$

From relationships (2), (3), (4), and (5), noting $i = \sigma\lambda$, it is found that

$$r = \frac{2\lambda_{N_{1s}}}{t}\left[1 + 2\frac{\exp(-t/\lambda_{N_{1s}})}{1 - \exp(-t/\lambda_{N_{1s}})}\right]^{-1}. \quad (6)$$

Cubes. Insofar as $\lambda_{Al_{2p}}$ and $\lambda_{N_{1s}}$, respectively, equal to 14 and 17 Å (*14*), are much smaller than the dimension a of the model considered, which is the case with our samples, the calculation of $I\,Al_{2p}$ and $I\,N_{1s}$ may be approximated fairly simply.

One considers that the Al_{2p} signal originates exclusively from a surface layer of equivalent thickness $\lambda_{Al_{2p}}$ in which there is no attenuation due to inelastic processes and that the N_{1s} signal is due to pyridine adsorbed on the three upper faces of the cube.

Developments similar to those previously described for the sheet model lead to

$$r = \frac{6\lambda_{N_{1s}}}{a}\sin 36°. \quad (7)$$

Spheres. The volume contributing to the Al_{2p} line for the sphere model is equal to the volume of the sphere minus the volume interpenetrated by an identical sphere displaced by a length $\lambda_{Al_{2p}}$ along Z (Fig. 2), i.e.,

$$\frac{4}{3}\pi R^3 - \frac{2\pi}{3}\left(R - \frac{\lambda_{Al_{2p}}}{2}\right)^2\left(2R + \frac{\lambda_{Al_{2p}}}{2}\right).$$

If it is considered that pyridine contributing to the N_{1s} line is adsorbed on the surface of the upper hemisphere, the following relationship is found:

$$r = \frac{3\lambda_{N_{1s}}}{2R^3}\left(R^2 - \frac{\lambda_{Al_{2p}}{}^2}{12}\right). \quad (8)$$

The r values calculated for the three models by relationships (6), (7), and (8) are plotted in Fig. 3 as a function of ρS, which allows comparison of all types of solids. The different models give substantially different results; however, they show that the correction factor r, which must be applied for comparing intensities of XPS lines due, respectively, to surface and bulk species, is not lower than 0.4 for adsorbants which, for a true density of about 2.5 g/cm³, develop a surface area of ~250 m²/g.

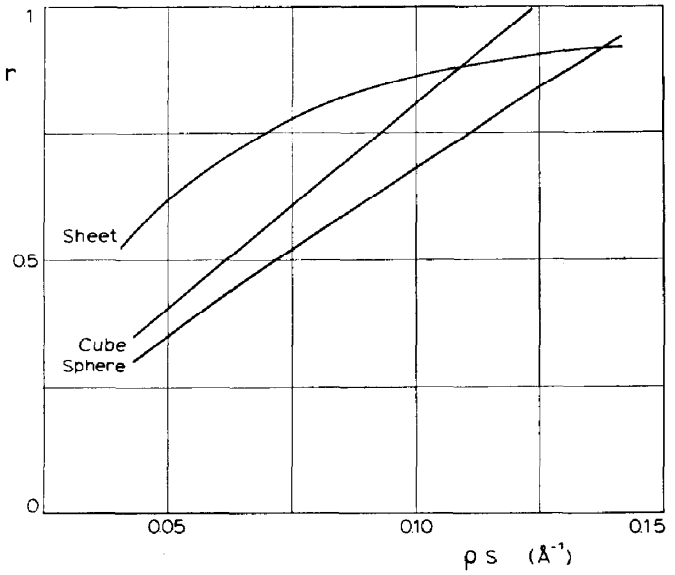

FIG. 3. Dependence of the correction factor r on the parameter ρS for different models.

Acidity Measurements

It has been mentioned before that the difference of $I\ N_{1s}/I\ Al_{2p}$ ratios between measurements on Py 100 and Bk 550 is a minimum estimate of the amount of chemisorbed pyridine. The concentration of acid sites, normalized per aluminum atom, has been calculated according to relations (2) and (6), thus using r values deduced from the sheet model. The surface areas are taken from Ref. (*9*) and the true specific weight ρ is calculated by interpolation between that of pure silica (2.2) and that of pure alumina (3.5). The $i_{Al_{2p}}/i_{N_{1s}}$ ratio has been taken equal to 0.36, which is the average of the values 0.33 and 0.40 proposed by Nefedov *et al.* (*12*) and Wagner (*13*), respectively.

The computed acid site concentration is presented in Fig. 4, which allows comparison with uncorrected results ($r = 1$). It should be pointed out that the model chosen for the correction is not critical at this level of accuracy; it is indeed shown by Fig. 3 that, the majority of the adsorbants considered here having ρS values not

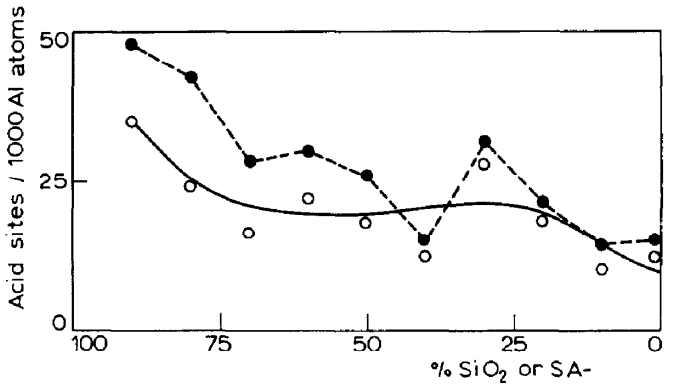

FIG. 4. Variation of acid site concentration (sites/1000 Al atoms) versus the silica content: (●----●) uncorrected data; (○——○) data corrected for the sheet model.

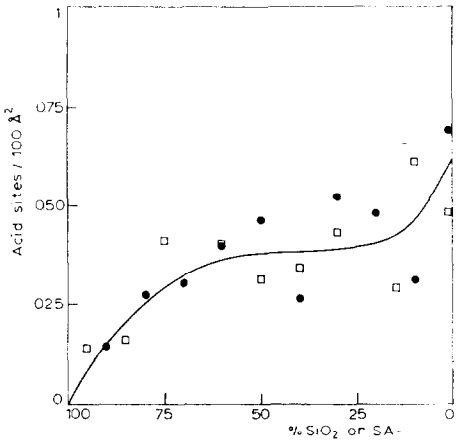

FIG. 5. Variation with silica content of the surface acid site density (sites/100 Å²): (●) XPS; (□) ir spectroscopy.

lower than ~0.07, r would not be lower than about 0.5, whatever the model.

The surface density of acid sites (sites per square nanometer) is given by

$$D \frac{C_{Al}}{S} \frac{N}{10^{20}},$$

where N is the Avogadro number. Scokart *et al.* (*3*) have measured the surface density of acid sites on the same samples by the ir study of the adsorption of pyridine. Coupling a microbalance with the ir spectrometer allowed them to determine selectively the amount of pyridine chemisorbed on Lewis and Brønsted sites. Fig. 5 shows that the agreement between XPS and ir spectroscopy is surprisingly good, considering the limited accuracy involved in both types of measurements.

The increase in surface acidity between 100 and 75% SiO_2 is attributed to the development of a mixed silica–alumina phase containing tetrahedral aluminum. The acid sites detected in that composition range are mainly OH groups (*2*, *3*). It has been found that between 75 and 50% SiO_2, the intrinsic properties of the surface do not change appreciably, but that increasing the Al_2O_3 content helps to increase the surface area (*9*). Below 50% SiO_2, the mixed phase is progressively diluted by alumina which appears as a distinct phase below 40–30% SiO_2; the latter is responsible for a further increase in the surface density of acid sites, which are Lewis sites.

Figure 4 shows that about one acid site is formed per 40 Al atoms and that the efficiency of aluminum to develop surface acidity decreases slightly as a function of the Al_2O_3 content.

The acidic hydroxyls responsible for the acidity at high SiO_2 contents are those which remained stable in the presence of atmospheric water or were recovered by pretreatment at high temperatures (*3*). The decrease in the number of acidic hydroxyls per Al atom as the SiO_2 content decreases from 100 to 70% suggests that the acidic surface hydroxyls are more stable or are recovered more easily when the concentration of acid sites generating Al atoms is small.

Si_{2p} Line

The total intensity I^t Si_{2p} of the Si_{2p} profile shown in Fig. 1, including the Si_{2p} line and the satellite line, has been measured for the four types of pretreatments. The average value I^t Si_{2p}/I Al_{2p} plotted versus C_{Si}/C_{Al} gives an excellent linear relationship for samples SA-100 to SA-30. According to relation (1), the slope corresponds to $i_{Si_{2p}}/i_{Al_{2p}}$, which is found to be equal to 1.79, as compared to literature values of 1.55 (*12*) and 1.56 (*13*). The agreement is better than for the ratio $i_{O_{1s}}/i_{Al_{2p}}$; this is due, as pointed out earlier, to the closer kinetic energy of the Al_{2p} and Si_{2p} lines. Below 30% SiO_2 the growing contribution of the satellite induces an increasing deviation.

In Fig. 6, the ratios I^t $Si_{2p}/(I^t$ Si_{2p} $+I$ $Al_{2p})$ and I $Al_{2p}/(I$ Al_{2p} $+ I^t$ $Si_{2p})$ are plotted versus the pseudoatomic fractions 1.79 $C_{Si}/(1.79$ C_{Si} $+$ $C_{Al})$ and $C_{Al}/(C_{Al}$ $+1.79$ $C_{Si})$, respectively, where 1.79 represents $i_{Si_{2p}}/i_{Al_{2p}}$. It should be kept in mind that XPS intensities do not allow one to

distinguish between a random mixture of particles of silica and alumina on the one hand and a completely homogeneous phase on the other hand; however, it is very sensitive to having one compound coated by the other. As the dots in Fig. 6 corresponding to SiO_2 contents higher than 30% fall on a straight line of unit slope, it may be concluded that there is no enrichment of either Al_2O_3 or SiO_2 near the surface of the grains constituting the powdered silica–alumina. If the mixed phase consisting of a silica network with aluminum substitution is coated by a layer of hydroxyaluminic cations, as suggested in the literature (*2*, *3*, *15*), the elementary particles formed in that way must be so small that the thickness of the coating does not exceed a monolayer.

Satellite Line

The complex satellite profile superposed on the Si_{2p} line is an energy-loss peak due to an interaction of the electrons originating from the Al_{2p} electronic level with the solid. This interpretation is supported by the fact that the O_{1s} line displays first- and second-order satellites (Fig. 1) characterized by the same energy loss (~25.1 eV).

The satellite can be considered as a fingerprint for the presence of a distinct alumina phase. Swanson (*16*) and Ditchfield (*17*) report similar spectra, with strictly identical shapes, for several alumina structures studied by energy-loss spectroscopy.

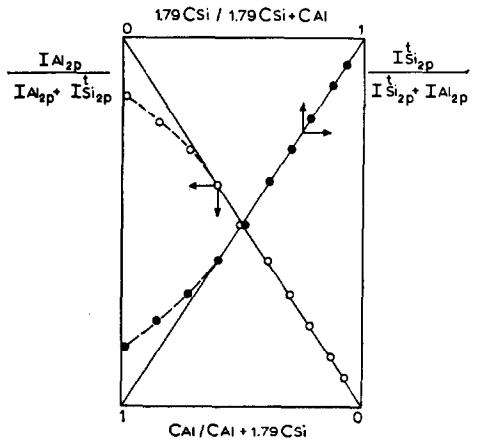

FIG. 6. Variation of Si_{2p} and Al_{2p} intensities versus the corresponding pseudoatomic ratios. Average of the four types of treatment.

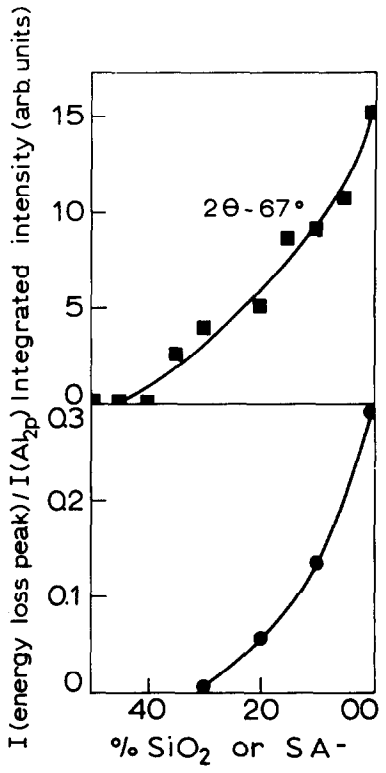

FIG. 7. Variation as a function of silica content of parameters characteristic of an alumina phase. Upper: area of the X-ray diffraction peak at $2\theta = 67°$ (CuK_α). Lower: Ratio of the intensity of the energy-loss peak to the Al_{2p} peak.

The energy-loss peak intensity referenced to that of the Al_{2p} line can be calculated using the relationship

$$\frac{I^{t}\,Si_{2p}}{I\,Al_{2p}} - 1.79\,\frac{C_{Si}}{C_{Al}}.$$

Its change as a function of the Al_2O_3 content (Fig. 7) follows closely the variation in the band at $2\theta = 67°$ (CuK_α) observed in the X-ray diffraction patterns of the silica–aluminas (*9*) and characteristic of an alumina phase. Our XPS results thus con-

firm that such a phase appears below 40–30% SiO_2.

CONCLUSIONS

Surface characterization of silica–aluminas by XPS has been conducted along two directions, namely, determination of the surface concentration in aluminum and silicon and characterization of the acidity.

Examination of Si_{2p} and Al_{2p} peaks has shown that there is no relative enrichment of SiO_2 or Al_2O_3 near the surface of the grains of the powdered silica–alumina. Between 100 and 30% SiO_2, the elementary particles having a silica-like network and presumably coated by hydroxyaluminic cations must be so small that the coating does not exceed a monolayer. On the other hand, the presence below 30–40% SiO_2 of an energy-loss peak characteristic of an alumina phase confirms the appearance of the latter only in that composition range.

Qualitative distinction between Brønsted and Lewis acidity by XPS was not successful for the silica–aluminas, contrary to what had been observed for zeolites (*10*). On the other hand, quantitative XPS determination of the total acidity compares well with the ir results obtained for the same systems. Provided that the precision of the XPS measurements is further improved, photoelectron spectroscopy can reveal itself as a competing technique for quantitative acidity measurements, especially when ir techniques are difficult, as, for instance, for solids of low surface area.

REFERENCES

1. Rouxhet, P. G. and Sempels, R. E., *J. C. S. Faraday Trans. I* **70**, 2021 (1974).
2. Sempels, R. E., and Rouxhet, P. G., *J. Colloid Interface Sci.* **55**, 263 (1976).
3. Scokart, P. O., Declerck, F. D., Sempels, R. E., and Rouxhet, P. G., *J. C. S. Faraday Trans. I* **73**, 359 (1977).
4. Parry, E. P., *J. Catal.* **2**, 371 (1969).
5. Kiselev, A. V., and Uvarov, A. V., *Surface Sci.* **6**, 399 (1967).
6. Pichat, P., Mathieu, M. V., and Imelik, B., *Bull. Soc. Chim. France* 2611 (1969).
7. Knözinger, H., and Kaerlein, C. P., *J. Catal.* **25**, 436 (1972).
8. Schwartz, J. A., *J. Vac. Sci. Technol.* **12**, 321 (1975).
9. Rouxhet, P. G., Scokart, P. O., Canesson, P., Defosse, C., Rodrique, L., Declerck, F. D., Leonard, A. J., Delmon, B., and Damon, J. P., "Colloid and Interface Science," Vol. 3, p. 81. Academic Press, New York, 1976.
10. Defosse, C., and Canesson, P., *J. C. S. Faraday Trans. I* **72**, 2565 (1976).
11. Ogilvie, J. J., and Wolberg, A., *Appl. Spectrosc.* **26**, 401 (1972).
12. Nefedov, V. I., Sergushin, N. P., Band, I. M., and Trzhaskovskaya, M. B., *J. Electron Spectrosc.* **2**, 383 (1973).
13. Wagner, C. D., *Anal. Chem.* **44**, 1050 (1972).
14. Friedman, R. M., *Silic. Ind.* **34**, 247 (1974).
15. Cloos, P., Leonard, A. J., Moreau, J. P., Herbillon, A., and Fripiat, J. J., *Clays Clay Miner.* **17**, 279 (1969).
16. Swanson, N., *Phys. Rev.* **165**, 1067 (1968).
17. Ditchfield, R. W., *Solid State Commun.* **19**, 443 (1976).